JOURNAL OF APPLIED ELECTROCHEMISTRY 18 (1988) 511–520

Characterization of electrochemically formed thin layers of binary alloys by linear sweep voltammetry

V. D. JOVIĆ

Institute of Technical Sciences of the Serbian Academy of Science and Arts, 11001 Beograd, P.O. Box 745, Yugoslavia

R. M. ZEJNILOVIĆ

Faculty of Metallurgy, University of Titograd, 81000 Titograd, Cetinjski put bb, Yugoslavia

A. R. DESPIĆ, J. S. STEVANOVIĆ

Faculty of Technology and Metallurgy, University of Beograd, 11000 Beograd, Karnegijeva 4, Yugoslavia

Received 13 July 1987; revised 1 December 1987

It has been demonstrated that linear sweep voltammetry can be used as an *in situ* technique for characterization of electrodeposited thin layers of binary alloys. The anodic dissolution characteristics of linear sweep voltammograms are very sensitive to the type of electrodeposited alloy. If both metals do not passivate in the investigated solution, eutectic type alloys are characterized by two sharp dissolution peaks, indicating no miscibility between components in the solid phase. From the ideal solid solutions, components of the alloy dissolve simultaneously, while in the case of intermediate phases and intermetallic compounds each phase, or compound, has its own peak of dissolution.

1. Introduction

It is known that electrodeposition offers several unique advantages in preparation of alloys (superior control of alloy composition, including formation of non-equilibrium alloys and the ability of formation of thin layers of alloys) and that electrochemically formed alloys may possess different characteristics than those obtained by metallurgical processes [1]. It has also been found that a change in the conditions of electrodeposition can cause a significant change in the phase structure of electrodeposits of identical chemical composition [2].

Characterization of electrochemically formed alloys by conventional techniques (SEM, X-ray diffraction, Auger spectroscopy, microprobe technique) is often connected with significant difficulties and is always a time consuming process. In this communication one possible *in situ* technique for characterization of electrochemically formed thin layers of binary alloys is presented. This is based on linear sweep voltammetry applied to the anodic dissolution of thin layers of alloys [3–7].

Three types of alloy were selected and investigated as examples of three different types of interaction between the components in the solid phase, according to their phase diagrams [8]: an alloy of a binary system with no miscibility (solubility) between components in the solid phase (eutectic type), an alloy with complete miscibility between components in the solid phase (solid solutions) and an alloy with formation of intermediate phases and/or intermetallic compounds.

Two procedures of investigation were applied to all three types of alloy. The first one involved a fixed glassy carbon disc electrode, while in the second one a rotating glassy carbon disc electrode was used. In the first procedure alloys were deposited and dissolved by a cathodic and anodic linear sweep of potential, respectively, in the solution containing ions of both metals. The second procedure consisted of deposition of a thin layer of an alloy (maximum thickness of about 1 μm) in the solution containing ions of both metals by potentiostatic pulse technique, followed by dissolution of the deposited alloy by anodic linear sweep voltammetry in the solution containing only ions of the less noble metal.

2. Experimental details

All experiments were carried out in standard electrochemical glass cells thermostated to 25 $\pm$ 1°C.

For the first procedure a mechanically polished glassy carbon (Atomergic Company) disc sealed in a Pyrex tube was used as a working electrode, a platinum plate as a counter electrode and a saturated calomel electrode (SCE, Radiometer K401) as a reference electrode.

The second procedure was performed in two cells, on the same mechanically polished glassy carbon disc electrode, sealed in a Kel-F rod by a special technique [9]. In the cell for deposition of a thin layer of alloy the counter electrode and the reference electrode were mode of chemically polished metal (99.999%) more noble of the two, while in the cell for the dissolution

0021-891X/88 $03.00 + .12

of electrochemically formed thin layer of the alloy, the counter and the reference electrode were made of chemically polished metal (99.999%) less noble of the two. The working electrode, with a deposited layer of alloy on it, was removed from the electrolyte under polarization, to prevent replacement. Thin layers of the alloys were deposited from appropriate baths [10].

Glassy carbon disc electrodes were first mechanically polished consecutively on emery papers of grade 0, 00, 000 and 0000 and then on polishing cloths (Buehler Ltd) impregnated with alumina (Banner Scientific Ltd) of 1 μm, 0.3 μm and 0.05 μm grades.

Prior to each experiment, solutions were deaerated inside the cell by purging with a stream of purified nitrogen [9]. All the solutions were made of p.a. chemicals and triply distilled water.

Linear sweep voltammetry was applied by using a potentiostat with built-in sweep generator (PAR-M273), while a potentiostatic pulse technique was applied by using a universal programmer (PAR-M175) and a potentiostat (Stonehart BC1200). Linear sweep voltammograms were recorded on an X–Y recorder (Philips PM8033), while potentiostatic j–t transients were recorded on an X–Y–t recorder (Houston Instrument 2000R).

Experiments with rotating disc electrodes were performed with Tacussel-Controvit rotating disc system.

3. Results

3.1. *The first procedure of investigation*

The linear sweep voltammograms (LSV) recorded on fixed glassy carbon disc electrodes in three different electrolytes containing (1) copper ions, (2) lead ions and (3) both ions in the same amounts (0.01 M), all in 1 M HBF_4, are shown in Fig. 1, together with the phase diagram of the binary alloy Cu–Pb [8]. It is seen that the LSV in electrolyte 3 corresponds reasonably well to the one which would be obtained by superposition of the LSVs pertaining to the electrolytes 1 and 2. This points to the complete absence of interaction between the two deposition processes and deposited metals. However, a small hump is observed between the two metal peaks which becomes higher after holding the working electrode at potentials negative to the reversible potential of lead, as can be seen in Fig. 2.

The LSVs of similar characteristics are shown in Fig. 3 for the solutions containing (1) cadmium ions, (2) zinc ions and (3) both ions in the same amounts (0.1 M), all in 0.5 M Na_2SO_4. Although both binary alloys are of the eutectic type, their phase diagrams are different, indicating possibilities of some interaction between cadmium and zinc in the solid phase [8].

The phase diagram of the Co–Pb alloy, shown in Fig. 4, indicates no miscibility between components in the solid phase, while the LSV of dissolution of alloy (curve 3) does not possess two separate peaks (Fig. 4).

In the case when the components in the solid phase make ideal solid solutions at all temperatures, like the system Cu–Ni (phase diagram [8] presented in Fig. 5), peaks of the dissolution of the components from the alloy are not separated (Fig. 5) as in Figs 1, 2 and 3. It is seen that nickel is passivated in the solution of 0.5 M Na_2SO_4 (curve 2) and that a small peak of dissolution of pure nickel could be seen on the voltammogram only after holding the potential at -0.75 V vs NHE for 300 s (curve 2a), but all deposited nickel was not dissolved. The two dissolution peaks present on curve 3 are the consequence of passivation of nickel in the sulphate solution. The first peak corresponds to dissolution of copper deposited on top of the nickel–copper layer during the anodic scan in the

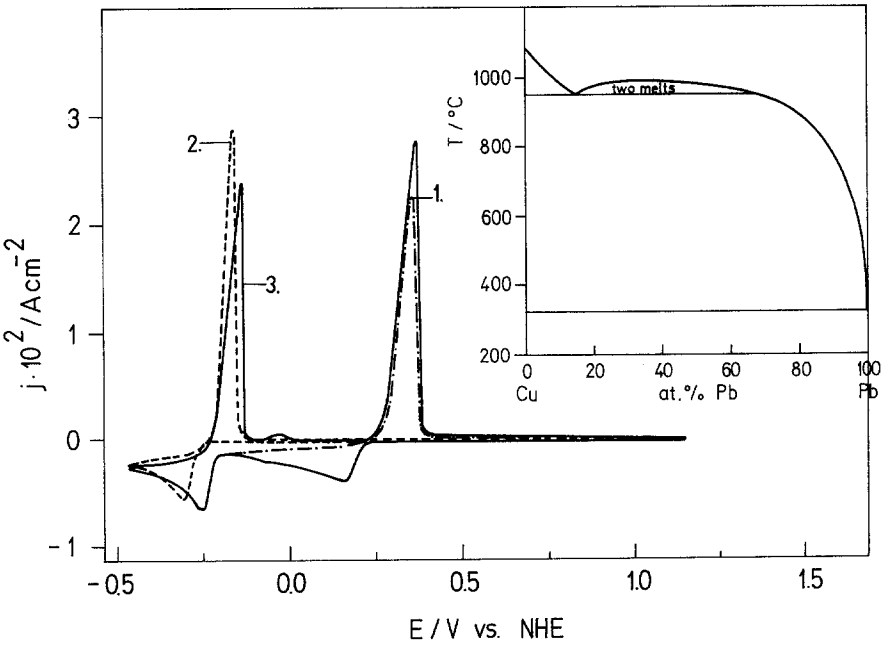

Fig. 1. Phase diagram of the Cu–Pb binary alloy and linear sweep voltammograms of a fixed glassy carbon electrode in various solutions: (1) 0.01 M Cu^{2+} + 1 M HBF_4; (2) 0.01 M Pb^{2+} + 1 M HBF_4; (3) 0.01 M Cu^{2+} + 0.01 M Pb^{2+} + 1 M HBF_4. Sweep rate, v = 50 mV s^{-1}.

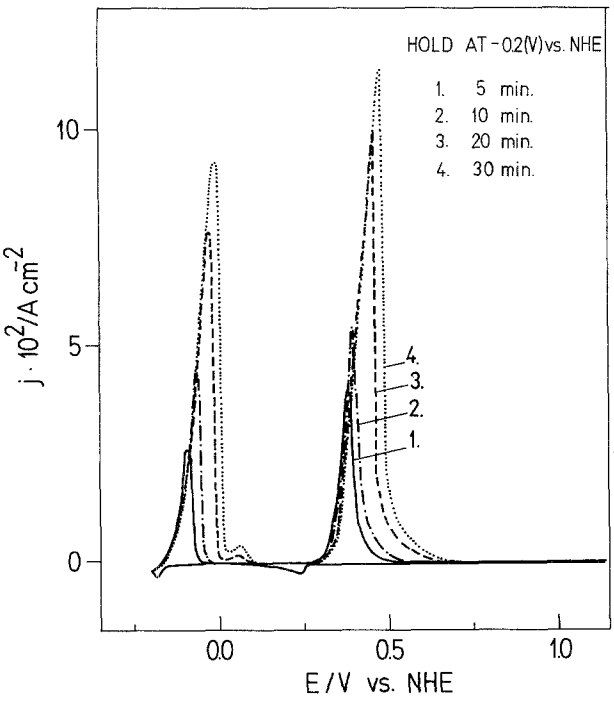

Fig. 2. Linear sweep voltammograms of dissolution of Cu-Pb alloy obtained by holding a fixed glassy carbon electrode at a potential of −0.2 V vs NHE in a solution containing 0.01 M Cu^{2+} + 0.01 M Pb^{2+} + 1 M HBF_4. Sweep rate, v = 10 mV s^{-1}.

cathodic region relative to the reversible potential of copper, while the second one corresponds to dissolution of the copper–nickel solid solution.

The LSVs of the systems with formation of intermediate phases and intermetallic compounds are shown in Fig. 6 for the solutions containing (1) copper ions, (2) zinc ions and (3) both ions of the same concentrations (0.1 M), all in the 0.5 M Na_2SO_4 and in Fig. 7 for the solutions containing (1) copper ions, (2) cadmium ions and (3) both ions of the same concentrations (0.1 M) in the electrolyte of 0.5 M Na_2SO_4 + 1 × 10^{-3} M H_2SO_4, together with their phase diagrams [8]. It is seen that LSVs of the system with intermediate phases (Cu–Zn) are different from those obtained for the system with intermetallic compounds (Cu–Cd). The deposition peak of zinc is shifted in a positive direction, while that of cadmium is not. On the other side, contrary to a relatively simple dissolution pattern in the system Cu–Zn, in the system Cu–Cd several anodic dissolution peaks are observed.

3.2. *The second procedure of investigation*

Potentiostatic j–t transients of deposition of thin layers of Cu–Pb alloy on rotating glassy carbon disc electrodes from the solution containing ions of both metals (0.05 M Cu^{2+} + 0.1 M Pb^{2+} + 1 M HBF_4) and the corresponding LSVs of dissolution of these alloys in the solution of lead ions (0.01 M Pb^{2+} + 1 M HBF_4) are presented in Fig. 8. It is seen that peaks of dissolution of lead and copper are separated and that a small hump appears after the dissolution peak of pure lead from the alloy, as was also observed in Figs 1 and 2.

Figure 9 represents potentiostatic j–t transients of deposition and corresponding LSVs of dissolution of thin layers of Cu–Ni alloys. The alloys were deposited from the solution of 0.05 M Cu^{2+} + 2 M Ni^{2+} + 0.5 M $Na_3C_6H_5O_7$ + 0.035 M NaCl and were dissolved in the chloride containing solution of Ni^{2+} ions (0.1 M $NiCl_2$ + 0.5 M NH_4Cl), to prevent passivation of deposited nickel. Curve 2 in Fig. 9(b) corresponds to dissolution of pure nickel, deposited from the Watts bath at the constant current.

Potentiostatic j–t transients of deposition and the

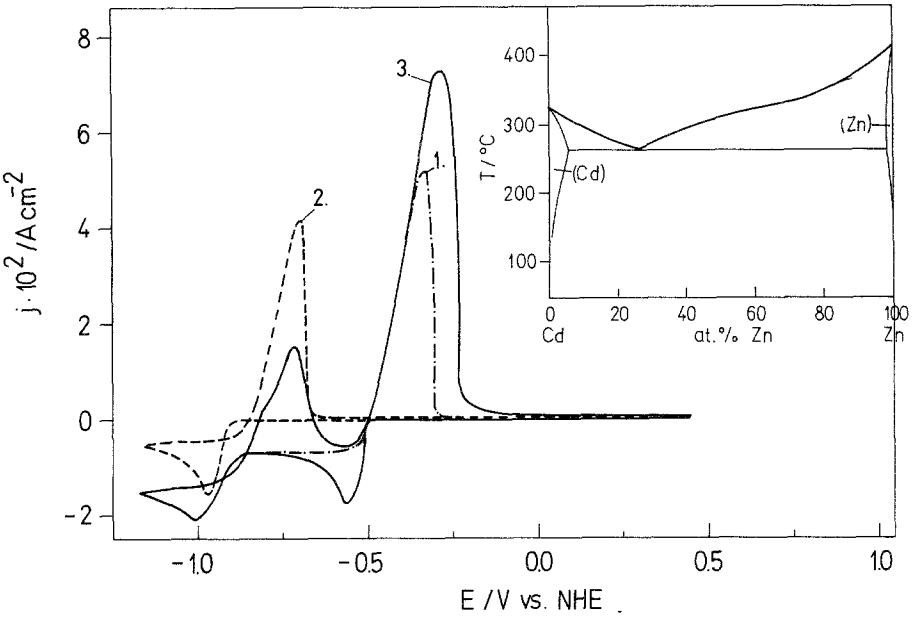

Fig. 3. Phase diagram of the Cd–Zn binary alloy and linear sweep voltammograms of a fixed glassy carbon electrode in various solutions: (1) 0.1 M Cd^{2+} + 0.5 M Na_2SO_4; (2) 0.1 M Zn^{2+} + 0.5 M Na_2SO_4; (3) 0.1 M Cd^{2+} + 0.1 M Zn^{2+} + 0.5 M Na_2SO_4. Sweep rate, v = 10 mV s^{-1}.

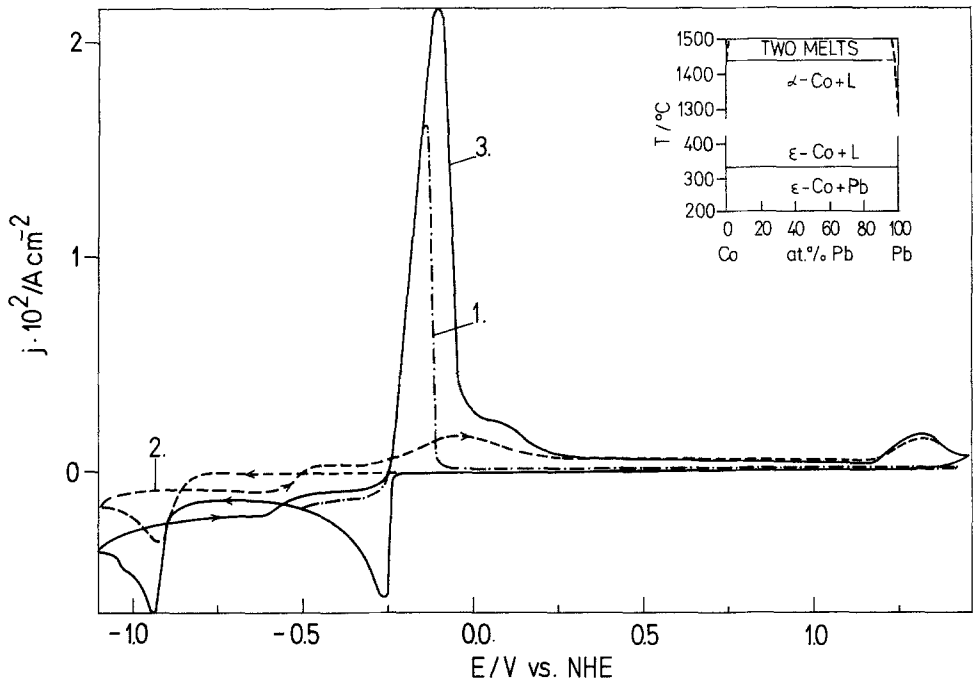

Fig. 4. Phase diagram of the Pb–Co binary alloy and linear sweep voltammograms of a fixed glassy carbon electrode in various solutions: (1) 0.01 M Pb^{2+} + 0.5 M $NaClO_4$ + 0.01 M $HClO_4$; (2) 0.01 M Co^{2+} + 0.5 M $NaClO_4$ + 0.01 M $HClO_4$; (3) 0.01 M Pb^{2+} + 0.01 M Co^{2+} + 0.5 M $NaClO_4$ + 0.01 M $HClO_4$. Sweep rate, $v = 50\,mV\,s^{-1}$.

corresponding LSVs of dissolution of thin layers of Cu–Zn and Cu–Cd alloys are shown in Figs 10 and 11. Thin layers of alloys were deposited from the solutions containing ions of both metals (Fig. 10(a), 0.01 M Cu^{2+} + 0.2 M Zn^{2+} + 0.5 M $(NH_4)_2SO_4$ + 0.05 M $[CH_2N(CH_2COOH)CH_2COONa]_2 \cdot 2H_2O$ and Fig. 11(a), 0.05 M Cu^{2+} + 0.2 M Cd^{2+} + 0.5 M Na_2SO_4 + 1×10^{-3} M H_2SO_4) and were dissolved in the solutions containing ions of the less noble metal (Fig. 10(b), 0.01 M Zn^{2+} + 0.5 M Na_2SO_4 and Fig. 11(b), 0.01 M Cd^{2+} + 0.5 M Na_2SO_4 + 1×10^{-3} M H_2SO_4). In the first system, at overpotentials at which a significant amount of zinc was deposited, the existence of three different structures, aside from the pure copper phase, is indicated by three peaks. The most actively dissolving structure was found to increase in quantity with increase of deposition overpotential. The second system gives a more complex dissolution pattern with a dominant peak at 0.5 V vs Cd^{2+}/Cd and with all peaks increasing with increasing deposition overpotential.

The LSV of dissolution of Cu–Cd alloy (curve 2),

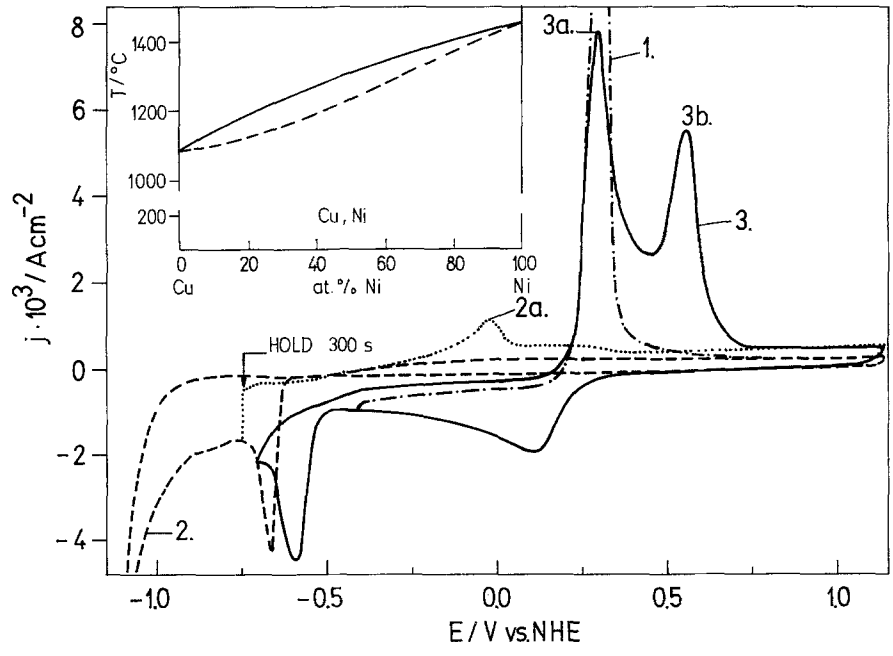

Fig. 5. Phase diagram of the Cu–Ni binary alloy and linear sweep voltammograms of a fixed glassy carbon electrode in various solutions: (1) 0.01 M Cu^{2+} + 0.5 M Na_2SO_4; (2) 0.01 M Ni^{2+} + 0.5 M Na_2SO_4; (3) 0.01 M Cu^{2+} + 0.01 M Ni^{2+} + 0.5 M Na_2SO_4. Sweep rate, $v = 10\,mV\,s^{-1}$.

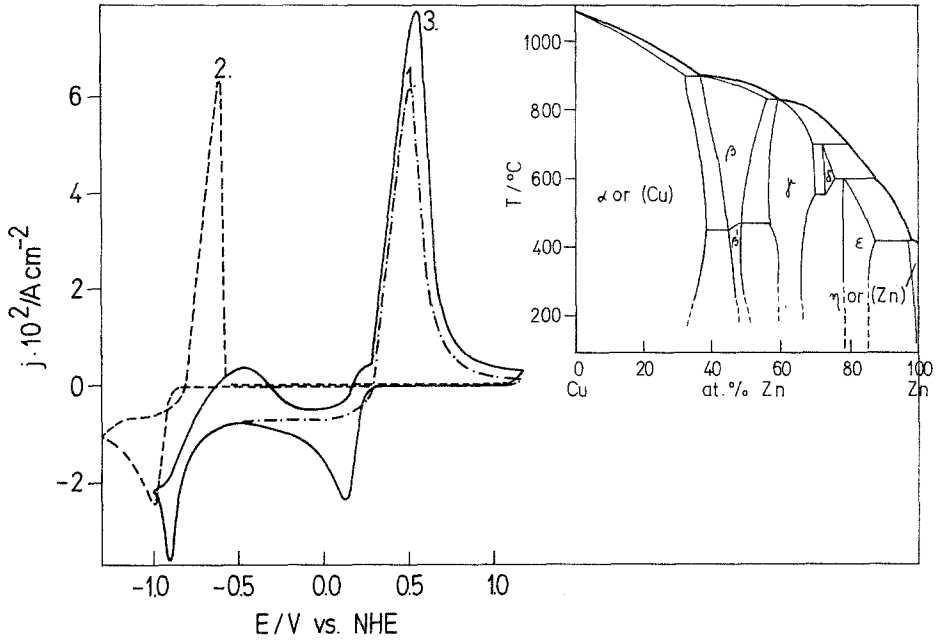

Fig. 6. Phase diagram of the Cu–Zn binary alloy and linear sweep voltammograms of a fixed glassy carbon electrode in various solutions: (1) 0.1 M Cu^{2+} + 0.5 M Na_2SO_4; (2) 0.1 M Zn^{2+} + 0.5 M Na_2SO_4; (3) 0.1 M Cu^{2+} + 0.1 M Zn^{2+} + 0.5 M Na_2SO_4. Sweep rate, v = 50 mV s^{-1}.

obtained from the solution containing 0.075 M Cu^{2+} + 0.2 M Cd^{2+} + 0.5 M Na_2SO_4 + 1 × 10^{-3} M H_2SO_4 at overpotential of −1.1 V vs Cu^{2+}/Cu for 20 s, is shown in Fig. 12 together with the LSV of dissolution of pure cadmium (curve 1). It is seen that four dissolution peaks, interpolated between the peaks of dissolution of pure cadmium and pure copper, are present on the voltammogram.

4. Discussion

4.1. *Eutectic type of alloys*

If the interaction between two components in the solid phase is negligible, the free energy of each component should not change and the reversible potential of each component in the alloy should be the same as the

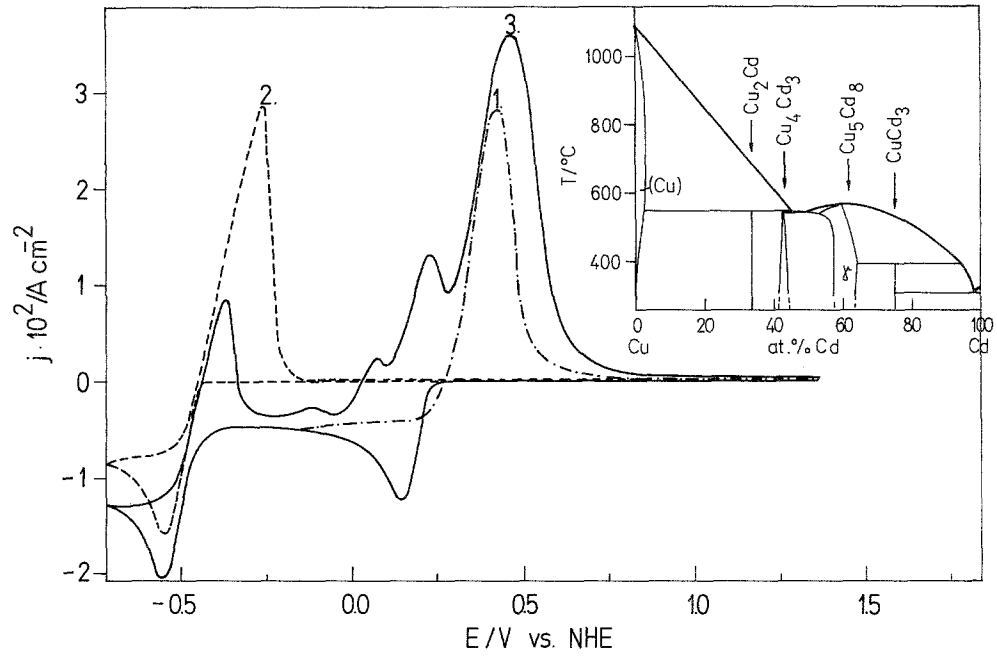

Fig. 7. Phase diagram of the Cu–Cd binary alloy and linear sweep voltammograms of a fixed glassy carbon electrode in various solutions: (1) 0.1 M Cu^{2+} + 0.5 M Na_2SO_4 + 1 × 10^{-3} M H_2SO_4; (2) 0.1 M Cd^{2+} + 0.5 M Na_2SO_4 + 1 × 10^{-3} M H_2SO_4; (3) 0.1 M Cu^{2+} + 0.1 M Cd^{2+} + 0.5 M Na_2SO_4 + 1 × 10^{-3} M H_2SO_4. Sweep rate, v = 50 mV s^{-1}.

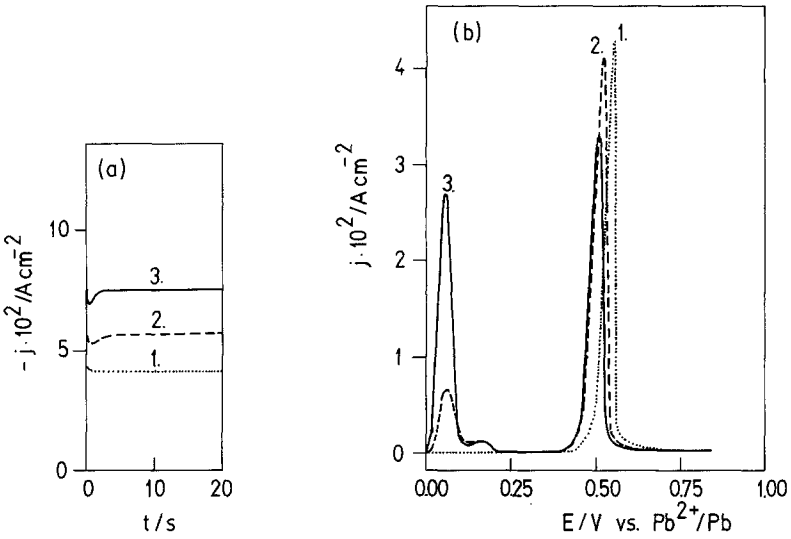

Fig. 8. Potentiostatic j–t transients of deposition (a) and corresponding linear sweep voltammograms of dissolution (b), of Cu–Pb alloy. (a) Solution: 0.05 M Cu^{2+} + 0.1 M Pb^{2+} + 1 M HBF_4; r.p.m. = 1000; (1) $\eta = -0.40$ V vs Cu^{2+}/Cu; (2) $\eta = -0.50$ V vs Cu^{2+}/Cu; (3) $\eta = -0.52$ V vs Cu^{2+}/Cu. (b) Solution: 0.01 M Pb^{2+} + 1 M HBF_4; r.p.m. = 1000; sweep rate, $v = 2\,mV\,s^{-1}$.

reversible potential of the pure component of the corresponding grain size. The anodic LSV of dissolution of such an alloy should possess only two separate peaks of dissolution of each component from the alloy [3, 4].

As can be seen in Figs 1–3 and 8, on the voltammograms of the Cu–Pb and Cd–Zn systems, two separate sharp peaks are observed which may be ascribed to separate dissolution of each component. When the applied potential of deposition is more positive than, or equal to -0.4 V vs Cu^{2+}/Cu, only copper is deposited on the rotating glassy carbon disc electrode. No further increase in current in the range of cathodic potentials from -0.2 to -0.4 V vs Cu^{2+}/Cu, proves that deposition is carried out at the diffusion limiting current density for copper ions (Fig. 8(a), j–t transient 1). On the LSV of such a deposit only one dissolution peak of pure copper is present (Fig. 8(b), curve 1). At higher overpotentials (j–t transients 2 and 3 of Fig. 8(a)), codeposition of lead commences and the dissolution LSV of such an alloy reflects this fact (curves 2 and 3 of Fig. 8(b)). The hump which appears on the voltammograms of Figs 1, 2 and 8 at some potential more positive than the reversible potential of lead is not unexpected, since the immiscibility of the two metals is not ideal. It is known from the literature that the solubility of solid lead in solid copper is very small in alloys obtained by metallurgical processes, but is about 10 wt % of Pb in electrodeposited alloys [11]. Accordingly, the hump may be attributed to some lead dissolved in solid copper. As can be seen in Fig. 2, this hump appears after holding the glassy carbon electrode at a potential negative to the reversible potential of lead for 20 min (curve 3) and becomes higher with increased amount of deposited lead and copper (curve 4).

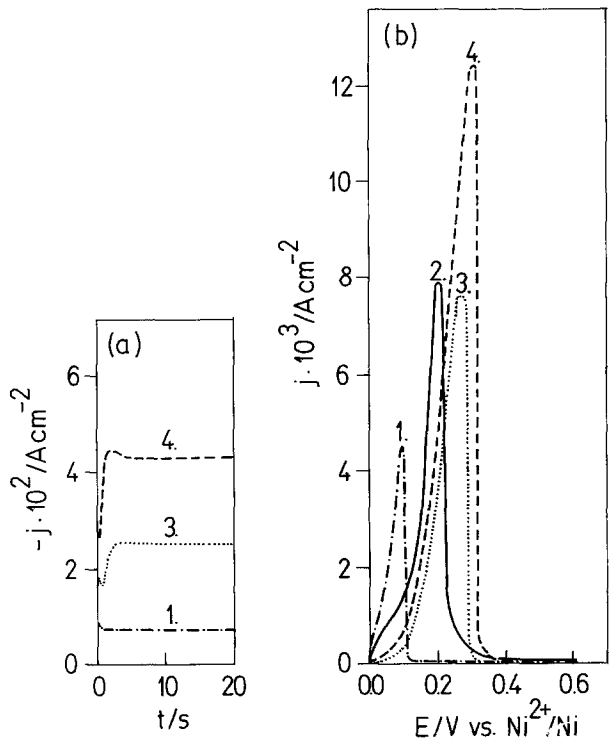

Fig. 9. Potentiostatic j–t transients of deposition (a) and corresponding linear sweep voltammograms of dissolution (b), of Cu–Ni alloy. (a) Solution: 0.05 M Cu^{2+} + 2 M Ni^{2+} + 0.5 M $Na_3C_6H_5O_7$ + 0.035 M NaCl; r.p.m. 1000; (1) $\eta = -0.60$ V vs Cu^{2+}/Cu; (3) $\eta = -1.10$ V vs Cu^{2+}/Cu; (4) $\eta = -1.20$ V vs Cu^{2+}/Cu. (b) Solution: 0.1 M Ni^{2+} + 0.5 M NH_4Cl; r.p.m. = 1000; sweep rate, $v = 2\,mV\,s^{-1}$. Curve 2 represents dissolution peak of pure nickel deposited from Watts bath.

Dissolution peaks of deposited metals are not always as sharp and reversible as in the voltammograms of Figs 1–3 and 8, because of possible passivation of deposited metals. In such a case and considering only the LSV of dissolution of a mixture of the two metals, one can come to a wrong conclusion concerning the nature of alloying. Such an example is shown in Fig. 4 for the system Pb–Co. It is seen that deposition of pure cobalt (curve 2) starts at about -0.75 V vs NHE, while dissolution of deposited cobalt commences at a potential more positive than that (about -0.5 V vs NHE) and takes place through two broad peaks.

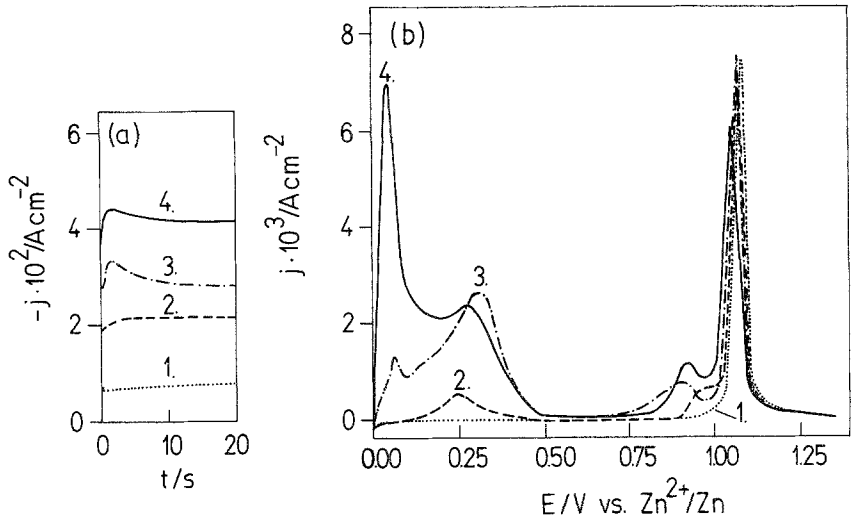

Fig. 10. Potentiostatic j–t transients of deposition (a) and corresponding linear sweep voltammograms of dissolution (b), of Cu–Zn alloy. (a) Solution: 0.01 M Cu^{2+} + 0.2 M Zn^{2+} + 0.5 M $(NH_4)_2SO_4$ + 0.05 M $[CH_2N(CH_2COOH)CH_2COONa]_2 \cdot 2H_2O$; r.p.m. = 1000; (1) $\eta = -0.80$ V vs Cu^{2+}/Cu; (2) $\eta = -1.10$ V vs Cu^{2+}/Cu; (3) $\eta = -1.14$ V vs Cu^{2+}/Cu; (4) $\eta = -1.17$ V vs Cu^{2+}/Cu. (b) Solution: 0.01 M Zn^{2+} + 0.5 M Na_2SO_4; r.p.m. = 1000; sweep rate, $v = 2\,mV\,s^{-1}$.

Because of such a dissolution characteristic of cobalt in the solution investigated, one may conclude (considering only the LSV of a mixture of two metals, curve 3) that lead and cobalt make an alloy more noble than either of the pure metals, which should not be possible according to their phase diagram and solubility data in the solid phase [12, 13].

4.2. *Solid solutions*

It has been calculated [14] that the injection of vacancies during dissolution of solid solutions is an unlikely process and it has been experimentally demonstrated earlier [15] that copper and nickel dissolve practically simultaneously from their solid solutions, although the difference between the standard potentials of pure metals is 0.575 V.

Recently, the theory of dissolution of different types of alloys has been developed [4], showing that the LSV of dissolution of solid solution should possess two separate (though not sharp) peaks, the first one corresponding to preferential dissolution of the less noble component at more negative potentials.

However, the experimentally recorded LSVs of dissolution of electrodeposited thin layers of copper–nickel alloys (Fig. 9(b) curves 3 and 4), contradict this theory. It is seen that dissolution of the copper–nickel alloys takes place through one peak only and that the peak potential of this dissolution is more positive than the peak potentials of dissolution of pure metals. This

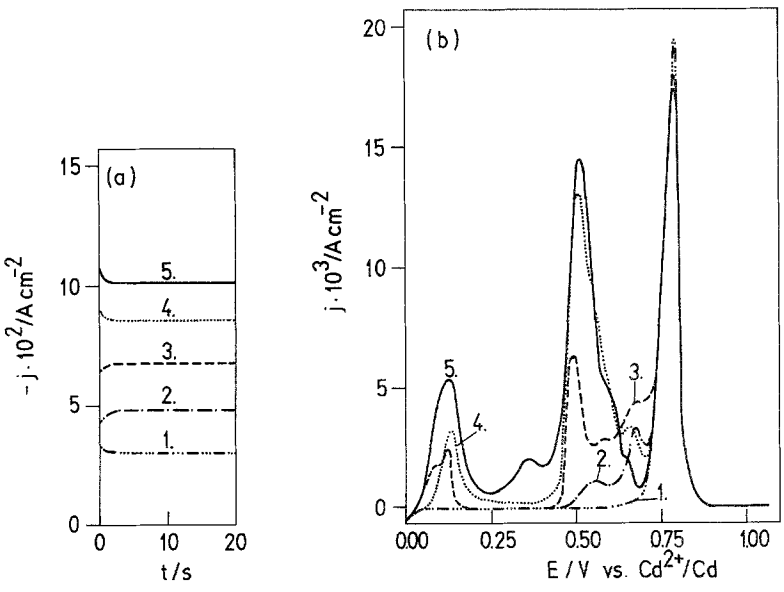

Fig. 11. Potentiostatic j–t transients of deposition (a) and corresponding linear sweep voltammograms of dissolution (b), of Cu–Cd alloy. (a) Solution: 0.05 M Cu^{2+} + 0.2 M Cd^{2+} + 0.5 M Na_2SO_4 + 1 × 10^{-3} M H_2SO_4; r.p.m. = 1000; (1) $\eta = -0.60$ V vs Cu^{2+}/Cu; (2) $\eta = -0.80$ V vs Cu^{2+}/Cu; (3) $\eta = -0.90$ V vs Cu^{2+}/Cu; (4) $\eta = -0.95$ V vs Cu^{2+}/Cu; (5) $\eta = -1.00$ V vs Cu^{2+}/Cu. (b) Solution: 0.01 M Cd^{2+} + 0.5 M Na_2SO_4 + 1 × 10^{-3} M H_2SO_4; r.p.m. = 1000; sweep rate, $v = 2\,mV\,s^{-1}$.

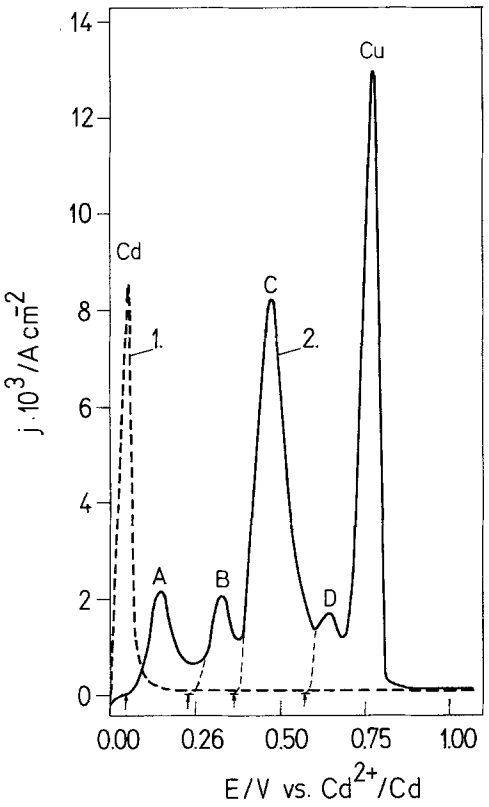

Fig. 12. Linear sweep voltammograms of dissolution of pure Cd (curve 1) and Cu–Cd alloy (curve 2) in the same solution as in Fig. 11(b), with sweep rate, $v = 1\,\mathrm{mV\,s^{-1}}$. Alloy was deposited at $\eta = -1.1$ V vs Cu^{2+}/Cu for 20 s with r.p.m. = 1000 in the solution containing 0.075 M Cu^{2+} + 0.2 M Cd^{2+} + 0.5 M Na_2SO_4 + 1×10^{-3} M H_2SO_4.

repeats the earlier finding [15] that copper and nickel dissolve simultaneously from their solid solutions and that the copper–nickel alloy is more noble than either of the pure metals.

It is known from the literature [16] that metal atoms in ideal solid solutions are completely randomly arranged and that solid solutions can contain short and long range order. However, some alloys, for example those in otherwise totally miscible copper and gold, possess 'superlattice' structures (CuAu and Cu_3Au superlattice). Knowing that atoms of copper and nickel are randomly arranged in their solid solutions [8], it is obvious that the dissolution LSV of such a solid solution should possess only one peak.

The peak potential being more noble than those of the components could be due to two causes: there could either be a significant free energy change in mixing, or some kinetic factor may cause the shift of the peak away from its reversible position in the positive direction. The ideal mixing in the Cu–Ni case, indicated by the phase diagram (Fig. 5), eliminates the first cause.

4.3. *Intermediate phases and/or intermetallic compounds*

The LSVs of dissolution of copper–zinc alloys are shown in Fig. 10(b). It is seen that the shape of the voltammogram depends on the amount of deposited zinc. At the overpotential of -0.80 V vs Cu^{2+}/Cu (j–t transient 1) only copper was deposited on the glassy carbon disc electrode and on the LSV of dissolution of that deposit only one peak of dissolution of pure copper, with the peak potential of 1.08 V vs the zinc reference electrode, is present. During the j–t transient 2, copper was deposited at its diffusion limiting current density and the deposited alloy contained about 66 at. % of zinc. According to the phase diagram of copper–zinc alloy (Fig. 6), alloy with 66 at. % of zinc should be characterized at low temperatures with two intermediate phases, β' and γ. The LSV of dissolution of that alloy (Fig. 10(b), curve 2), does possess two broad peaks which could be ascribed to dissolution of zinc from the two intermediate phases at potentials of about 0.25 and 0.97 V vs Zn^{2+}/Zn, the third peak pertaining to dissolution of copper. Such a large difference in the chemical potential of zinc in the two phases, with relatively small difference in copper content, is indeed difficult to understand. It may well be that even an α phase is formed under these conditions. As the amount of zinc in the electrodeposited alloy increases (75 at. % in curve 3 and 83 at. % in curve 4), these two peaks become more pronounced and one new peak appears at the beginning of dissolution of the alloys, which should correspond to the dissolution of zinc from the intermediate phase richest in zinc.

If the components of the alloy make intermetallic compounds, dissolution peaks on the LSVs are very well defined, as can be seen in Fig. 11(b), for the copper–cadmium alloy. The j–t transient 1 corresponds to the deposition of pure copper and on the LSV of dissolution only one peak is present. As the amount of cadmium in the alloy increases new peaks appear on the voltammograms, but the dissolution peak of copper remains almost the same.

The number and the height of peaks also depend on the amount of deposited copper. At lower concentrations of copper ions (a smaller amount of copper is deposited per unit time because the diffusion limiting current density is lower), the number of dissolution peaks is reduced, but peaks at more positive potentials (near the dissolution peak of copper) become more pronounced. If the amount of copper in the deposited alloy increases, the number of dissolution peaks increases (reaching a maximum number of four) and three of them become more pronounced, while the more positive one almost disappears.

A typical dissolution LSV of copper–cadmium alloy with more than 80 at. % of cadmium is shown in Fig. 12, curve 2. (The amount of deposited zinc and cadmium in at. % was obtained from the total charge under the transient reduced for the charge under the j–t transient of deposition of copper by its diffusion limiting current density.) In the same figure, the voltammogram of dissolution of pure cadmium is presented by curve 1. Four separate peaks (A, B, C and D), interpolated between the peaks of dissolution of pure cadmium and pure copper, may be ascribed to the dissolution of cadmium from four different intermetallic compounds marked on the phase diagram in Fig. 7.

Table 1. Calculated amounts of copper contained in the deposited Cu–Cd intermetallic compounds

Peak	*Assumed formula*	*Charge of dissolved Cd* ($C\,cm^{-2}$)	*Calculated charge of Cu* ($C\,cm^{-2}$)	*Total charge of Cu* ($C\,cm^{-2}$)
Cu	Cu	–	0.850	0.850
A	$CuCd_3$	0.213	0.071	1.697
B	Cu_5Cd_8	0.170	0.106	
C	Cu_4Cd_3	0.942	1.256	
D	Cu_2Cd	0.132	0.264	

It is logical to assume that the increase in the noble character of cadmium in the compound parallels the increase in the copper content. Hence, the peaks from A to D should reflect the presence of the compounds in the order $CuCd_3$, Cu_5Cd_8, Cu_4Cd_3 and Cu_2Cd.

If this assumption is valid, the same charge as that under the copper peak should be obtained from the sum of charges under the cadmium dissolution peaks multiplied by the corresponding stoichiometric ratios (copper to cadmium) arising from the formulae. The result is seen in Table 1. It is found that the sum of charges almost exactly doubles that obtained from the copper peak. This was calculated, however, assuming that copper dissolves exchanging 2 electrons per atom. The figures, thus, indicate that only one electron per atom should be taken for the calculation of the sum. This is not unexpected since it is known that copper dissolution occurs in two steps, the second step necessitating the presence of cuprous ions in the reaction layer. In the rotating disc experiment, cuprous ions are likely to be swept away before they are further oxidized.

Furthermore, a question arises as to whether all the phases are present in the alloy as deposited, or, as suggested by Swathirajan [4], the alloy may consist initially of a single phase, richest in cadmium, and subsequent phases are obtained by phase transition during the anodic sweep (as the cadmium content is decreased). If the latter was the case, a rational relationship between charges under different peaks (pertaining to gradual release of cadmium) should exist till only copper remained in the deposit. Thus, if the stoichiometry of the known compounds is $CuCd_3$, Cu_5Cd_8, Cu_4Cd_3 and Cu_2Cd, and transformation from one into the other took place, the ratio between the charges under the peaks should be 1 : 0.607 : 0.179 : 0.347. Since such a relationship was not found experimentally, the result indicates that all the phases are present in the sample independently of each other and before the start of the anodic sweep.

It is interesting to note that the shape and the height of the peaks depend on the time spent at open circuit in the nitrogen atmosphere before dissolution. The LSV presented in Fig. 12 is obtained immediately after deposition, but if deposited alloy is left at open circuit in a nitrogen atmosphere for 15 min, the peak A disappears and the peak B becomes higher. It is obvious that immediately after the deposition, the alloy is in a meta-stable state and hence tends to achieve a lower free energy, i.e. the stable equilibrium state, by some solid state reaction. This is being investigated, together with the influence of the amount of deposited copper on the shape of alloy dissolution voltammograms and the results will be reported later.

It is known that often the configuration of atoms that has the minimum free energy after mixing does not have the same crystal structure as either of the pure components and that this new structure is known as an intermediate phase. The difference between the intermediate phase and the intermetallic compound is not in their structures, but in the change of their free energies with composition. When small composition deviations cause a rapid rise in free energy, the phase is known as an intermetallic compound. The intermediate phases do not have such a sharp change in free energy with composition [16], as it is schematically presented in Fig. 13. This means that the reversible potential of the less noble metal in the intermetallic compound is a singular point, while in the intermediate phase it is not well defined and depends on the change of the free energy with composition. This could be the reason why the dissolution peaks of the less noble metal from intermetallic compounds are much sharper than the dissolution peaks of the same compound if it had the character of an intermediate phase.

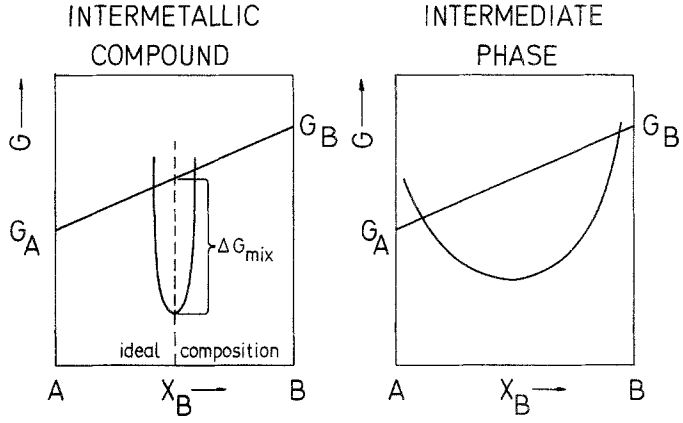

Fig. 13. Schematic representation of a change of the free energy with composition for intermetallic compound and intermediate phase.

Table 2. Reversible potentials, free energy changes of cadmium entering different intermetallic compounds and activity of cadmium in the intermetallic compounds

Formula of intermetallic compound	*Reversible potential (V vs Cd^{2+}/Cd)*	*Free energy of formation ($kJ\,mol^{-1}$)*	*Activity ($mol\,dm^{-3}$)*
Cu_2Cd	0.57	−110.0	5.8×10^{-20}
Cu_4Cd_3	0.36	−69.5	6.8×10^{-13}
Cu_5Cd_8	0.22	−42.5	3.8×10^{-8}
$CuCd_3$	0.05	−9.6	2.1×10^{-2}

4.4. *Reversible potential and the free energy change of cadmium in the formation of intermetallic compounds*

The reversible potential of cadmium metal in the solution of its ions, E_r^{Cd}, which is, in our experiments, the potential of the reference electrode, is given by the Nernst equation

$$E_r^{Cd} = E_{r,0}^{Cd} + \frac{RT}{2F} \ln a_{Cd^{2+}} \quad (1)$$

where $E_{r,0}^{Cd}$ is the standard potential of cadmium and $a_{Cd^{2+}}$ is the activity of cadmium ions in the solution; the activity of pure metal being taken as unity.

The reversible potential of cadmium in the intermetallic compound, $E_{r,all}^{Cd}$, is given by the equation

$$E_{r,all}^{Cd} = E_{r,0}^{Cd} + \frac{RT}{2F} \ln \frac{a_{Cd^{2+}}}{a_{Cd,all}} \quad (2)$$

(it is assumed that the surface free energy contribution at the interface alloy/electrolyte is negligible) where $a_{Cd,all}$ is the activity of cadmium in the intermetallic compound.

The difference between the two reversible potentials, ΔE, is given as

$$-\Delta E = E_r^{Cd} - E_{r,all}^{Cd} = \frac{RT}{2F} \ln a_{Cd,all} \quad (3)$$

and from this

$$-2F\Delta E = RT \ln a_{Cd,all} = \Delta G_{all} \quad (4)$$

where ΔG_{all} is the free energy of formation of the intermetallic compound.

As a first approximation, by extrapolating the rising portion of the anodic current of the peaks (as it is schematically presented in Fig. 12) to the potential axis, using Equations 3 and 4 it was possible to calculate the reversible potential and the free energy of formation of the intermetallic compounds and the activity of cadmium in these compounds. The result of such a calculation is presented in Table 2.

Acknowledgements

The authors are indebted to the National Science Foundation (USA), to the Research Fund of S. R. Serbia and the Research Fund of S. R. Montenegro for financial support of this work.

References

[1] A. Brenner, 'Electrodeposition of Alloys, Principles and Practice', Academic Press, New York (1963).
[2] M. H. Gelshinski, L. Gal-Or and J. Yahalom, *J. Electrochem. Soc.* **129** (1982) 2433.
[3] R. M. Zejnilović and V. D. Jović, 4th Yugoslav Symposium of Analytical Chemistry, Split, Yugoslavia (1985), 'Book of Abstracts', p. 172.
[4] S. Swathirajan, *J. Electrochem. Soc.* **133** (1986) 671.
[5] R. M. Zejnilović and V. D. Jović, 29th Symposium of Serbian Chemical Society, Beograd, Yugoslavia (1987), 'Book of Abstracts', p. 124.
[6] V. D. Jović, R. M. Zejnilović, A. R. Despić and J. S. Stevanović, 10th Yugoslav Symposium of Electrochemistry Bečići, Yugoslavia (1987), 'Extended Abstracts', p. 358.
[7] V. D. Jović, R. M. Zejnilović, A. R. Despić and J. S. Stevanović, 38th ISE Meeting, Maastricht, Netherlands (1987), 'Extended Abstracts', Vol. I, p. 383.
[8] M. Hansen and K. Andrenko, 'Constitution of Binary Alloys', McGraw-Hill, New York, Toronto, London (1958).
[9] J. N. Jovićevic, V. D. Jović and A. R. Despić, *Electrochim. Acta* **29** (1984) 1625.
[10] V. V. Bondar, V. V. Grimina and V. N. Pavlov, Itogi nauki i tehniki, Electrokhimiya, Moskow (1980) Vol. 16.
[11] E. Raub and A. Engel, *Z. Metallkunde* **41** (1950) 485.
[12] G. Tammann and W. Oelsen, *Z. anorg. Chem.* **186** (1930) 279.
[13] E. Pelzel, *Metall.* **9** (1955) 692.
[14] D. A. Vermilyea, *J. Electrochem. Soc.* **115** (1968) 143.
[15] J. O. M. Bockris, B. T. Rubin, A. Despić and B. Lovreček, *Electrochim. Acta* **17** (1972) 973.
[16] D. A. Porter and K. A. Easterling, 'Phase Transformations in Metals and Alloys', Van Nostrand Reinhold, Wokingham (1980).